Acta Cryst. (1974). A30, 448

Use of a Two-axis Neutron Diffractometer on an Angled Reactor Channel

BY B. C. G. HAYWOOD

A.E.R.E., Harwell, Didcot, Berkshire, England

(*Received* 10 *May* 1973; *accepted* 2 *January* 1974)

The resolution function is derived for a two-axis neutron diffractometer in which the monochromator scattering plane is inclined to the specimen scattering plane. The analysis shows that useful results can be obtained from powder diffractometers which operate in the horizontal plane and are installed on reactor holes inclined by up to 35° from the horizontal. It is also shown that single-crystal diffractometers may be installed on reactor holes with angles up to 50° from the horizontal.

Introduction

The use of thermal neutrons from high-flux reactors has increased over the past few years to the point where the demand cannot be met by the use of the limited number of available horizontal beam channels. Attention has therefore been turned to the possibility of using the angled channels which are installed on these reactors. It is widely believed that only a diffractometer with monochromator and analyser scattering planes parallel will have a satisfactory resolution function and the difficulties in designing such an instrument to work on an angled channel are very great. It is the purpose of this paper to show that in some cases the resolution function of a diffractometer in which these planes are not parallel can still be attractive. Thus it is quite feasible to build a diffractometer for use on an angled reactor channel in which the monochromator produces a horizontal beam of neutrons and the second and subsequent scattering processes take place in the horizontal plane.

The resolution function of the normal two-axis diffractometer has been considered by several authors and may be said to be well understood. Two methods of calculation are possible. In the first method originally used by Caglioti, Paoletti & Ricci (1958, 1960) the calculation is carried out in real space and the result is a distribution of doubly scattered neutrons as a function of counter and specimen angle. In the second method adopted by Cooper & Nathans (1968) (CN) the calculation is carried out in reciprocal space and the result is an exponential distribution of probability of neutron transmission as a function of **Q**, the momentum transferred to the neutron from the system during the collision. This distribution may then be used to evaluate the distribution of scattered neutrons for any type of specimen.

The real-space method is the simpler both to visualize and to evaluate but it suffers a little from a lack of flexibility in that different calculations have to be made according to whether the case under consideration is a powder or a single-crystal diffractometer. The reciprocal-space method of calculation is more complex but it produces a resolution function which can be interpreted for any type of specimen or mode of operation of the diffractometer. It also gives an insight into what is actually happening in reciprocal space as the various parameters of the instrument are varied. This method will be used in the present report.

The resolution function

The resolution function will be derived exactly as in the Cooper–Nathans calculations with the addition of terms in the direction normal to the specimen scattering plane. The arrangement of the diffractometer is shown in Fig. 1. Neutrons emerge from the reactor at an angle ψ to the horizontal plane, pass through a collimator C_0 and strike the monochromator M. At this point those with mean wavelength λ which satisfy the Bragg condition are scattered through an angle $2\theta_M$ into the horizontal plane. After passing through collimators C_1' and C_1 the beam of neutrons strikes the specimen and those passing through collimator C_2 at a mean angle $2\theta_s$ to the monochromator–specimen direction in the horizontal plane are detected by the counter.

In the evaluation C_0 and C_1' are considered to have divergences $\alpha_0\alpha_1'$ and $\beta_0\beta_1'$ in and perpendicular to the monochromator scattering plane and C_1 and C_2 have divergences $\alpha_1\alpha_2$ and $\beta_1\beta_2$ in and perpendicular to the specimen scattering plane respectively.

The resultant picture in reciprocal space is given in Fig. 2. An initial beam of neutrons with most probable wave vector $\mathbf{k}_0$ is scattered by the monochromator M through an angle $2\theta_M$ into the horizontal plane. In the horizontal plane the beam of neutrons from the monochromator with most probable wave vector $\mathbf{k}_I$ is scattered through an angle $2\theta_s$ by the specimen and finally the resulting beam with most probable wave vector $\mathbf{k}_F$ is passed through to the detector. This diagram is exactly Fig. 2 of Cooper & Nathans with the first scattering plane rotated through an angle φ about $\mathbf{k}_I$. We shall define $\mathbf{Q}$ as $\mathbf{k}_F-\mathbf{k}_I$, $\mathbf{k}_0$, $\mathbf{k}_i$ and $\mathbf{k}_f$ are wave vectors corresponding to any elastic scattering process ($|\mathbf{k}_i|=|\mathbf{k}_0|=|\mathbf{k}_f|=k$) and $\Delta\mathbf{k}_i=\mathbf{k}_i-\mathbf{k}_I$, $\Delta\mathbf{k}_f=\mathbf{k}_f-\mathbf{k}_F$. $\Delta\mathbf{Q}=\mathbf{k}_f-\mathbf{k}_i-\mathbf{Q}$.

It can then be shown that the probability of a neutron being transmitted through the system is given by

$$P(\mathbf{k}_i,\gamma_1,\gamma_1',\gamma_2,\delta_1,\delta_1',\delta_2)$$
$$\propto \exp -\tfrac{1}{2}\left\{\frac{[(\Delta k_i/k_i)\tan\theta_M+\gamma_1]^2}{\eta_M^2}\right.$$
$$+\frac{[2(\Delta k_i/k_i)\tan\theta_M+\gamma_1]^2}{\alpha_0^2}+\frac{\gamma_1^2}{\alpha_1'^2}+\frac{\gamma_1'^2}{\alpha_1^2}+\frac{\gamma_2^2}{\alpha_2^2}$$
$$\left.+\frac{\delta_1^2}{4\sin^2\theta_M\eta_M'^2+\beta_0^2}+\frac{\delta_1^2}{\beta_1'^2}+\frac{\delta_1'^2}{\beta_1^2}+\frac{\delta_2^2}{\beta_2^2}\right\} \quad (1)$$

where $\gamma_1'\gamma_2$ and $\delta_1'\delta_2$ are the horizontal and vertical divergence angles with respect to the optimum directions in the scattering plane and γ_1 and δ_1 are the divergence angles in the monochromator plane, θ_M is the monochromator Bragg angle and η_M and η_M' are the horizontal and vertical monochromator mosaics respectively. It is assumed that C_1 and C_1' are completely independent. In equation (1) γ_1' and δ_1' may be expressed in terms of γ_1 and δ_1 and the equation becomes a function of five variables. By substitution of the components of $\Delta\mathbf{Q}$ for the components of $\Delta\mathbf{k}_i$, γ and δ and performing two integrations as described in Appendix B, it is possible to arrive at a three-dimensional function $R(\mathbf{Q}+\Delta\mathbf{Q})$ expressed in terms of the components of $\Delta\mathbf{Q}$. This function has the form

$$R(\mathbf{Q}+\Delta\mathbf{Q})=R_0\exp -\tfrac{1}{2}\Big(\sum_{k=1}^{3}\sum_{l=1}^{3}X_kA_{kl}X_l\Big) \quad (2)$$

where X_1, X_2 and X_3 are ΔQ_x, ΔQ_y, ΔQ_z the deviations of $\mathbf{Q}$ along the line of $\mathbf{Q}$ and at right angles to $\mathbf{Q}$ in and perpendicular to the scattering plane respectively.

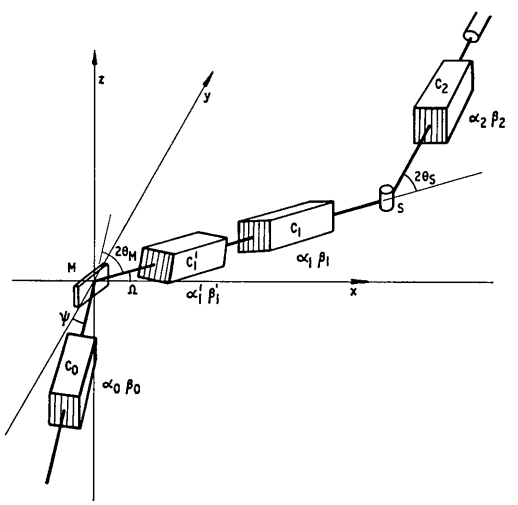

Fig. 1. The experimental arrangement. Collimators C_0 and C_1' are in the monochromator scattering plane while collimators C_1 and C_2 are in the specimen scattering plane. Divergences α and β are respectively parallel and perpendicular to the scattering planes.

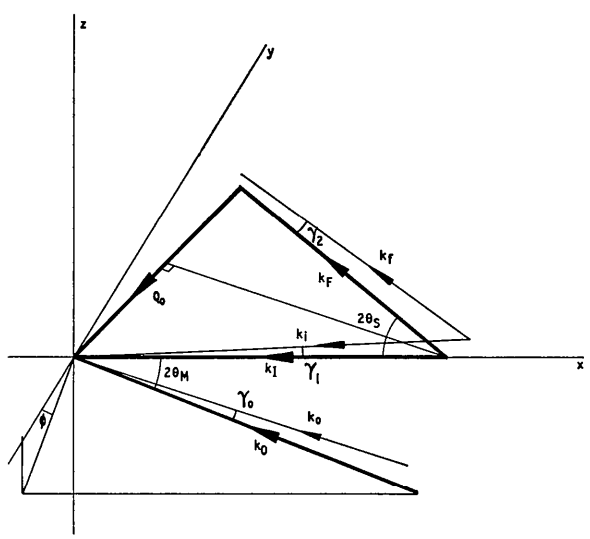

Fig. 2. The reciprocal-space diagram of the experimental arrangement of Fig. 1.

Discussion of instrumental resolution

The form of the resolution function can be seen to be an exponential function whose exponent is a homogeneous function of $\mathbf{Q}$ of order two. Thus if we equate the exponent to some value p we define the locus of points in $\mathbf{Q}$ space for which the resolution function has a value $R_0\exp -(p/2)$. This locus can be seen to be an ellipsoid. It is therefore convenient to visualize the resolution function by considering the locus of points for which the probability is $R_0/2$, *i.e.* $p=1{\cdot}386$.

Having derived this locus of probability $=\frac{1}{2}$ it may now be used to predict actual line widths observed under experimental conditions. The simplest case to consider is the powder diffractometer. The reciprocal-space diagram for a powder is a concentric set of spheres and the action of the spectrometer in making measurements at constant $\mathbf{k}_0$ at increasing values of θ_s is to pass the probability distribution through each diffraction sphere normal to the radius. The count rate of the neutron detector can be evaluated at each value of θ_s by integrating the probability distribution of equation (2) on the surface of the sphere. This calculation may be further simplified by assuming that the probability ellipsoid has significant values only for $\Delta\mathbf{Q}$ much smaller than the radius of the diffraction sphere. It may be easily shown that the resulting count rate is a Gaussian function of θ_s with half values at the points at which the surface of the ellipsoid with probability $=R_0/2$ is tangential to the diffraction sphere.

The second case to be considered is the single-crystal diffractometer in the ω scan mode with only the crystal rotating and with the counter at a fixed angle. A perfect crystal has a reciprocal-space diagram consisting of a series of delta functions and, if the detector is correctly set up, one of these delta functions passes through the centre of the resolution ellipsoid on the arc of a circle with the reciprocal-lattice zero point as its centre. Making the same approximation as to the relative sizes of $\mathbf{Q}$ and $\Delta\mathbf{Q}$ we see that the angular half width observed is given by $2{\cdot}35/(M_{22})^{1/2}k\sin\theta)$.

The third case is the θ–2θ scan in which the crystal is rotated through θ while the counter is moved through 2θ. This has the effect of moving the resolution ellipsoid along **Q** and if its centre passes over a reciprocal-lattice point on the specimen diagram the resulting peak has width $2{\cdot}35/(M_{11})^{1/2}k\cos\theta$).

The use of single-crystal specimens with a significant mosaic spread will modify these derivations somewhat since instead of being a delta function in reciprocal space the lattice point is now a probability distribution forming a small part of a sphere of radius τ. If the mosaic of the specimen has angular half width in the horizontal plane h the width of the curve with only the specimen rotating can be easily seen to be

$$\left(\frac{5{\cdot}52}{M_{22}k^2\sin^2\theta}+h^2\right)^{1/2}.$$

In the case of the θ–2θ scan the result is not so readily seen as one pushes the resolution ellipsoid through the probability distribution the value of half width must be evaluated from an integration of the product of the resolution and mosaic distribution over the three dimensions.

Calculated results

(i) *Powder diffractometer*

The calculated resolution widths of a powder diffractometer are shown in Fig. 3 as a function of the angle φ between the monochromator and scattering planes. The parameters chosen for this example are typical of those of a medium resolution diffractometer such as the PANDA instrument at A.E.R.E. The effect of increasing the interplanar angle is to reduce the effect of focusing by increasing the value of the minimum resolution width and at the same time shifting the minimum to smaller scattering angles θ_s. For the parameters given in Fig. 3 it can be seen that the resolution obtained for $\varphi=35°$ although worse than that for $\varphi=0°$ is still quite acceptable for this type of instrument. Improvement of the resolution in this case to comparable values to those of $\varphi=0$ can be obtained by reducing α_0, α_2 and β_1 to values of 12, 7 and 30′ where the transmitted intensity is 0·28 of that for the $\varphi=0$ instrument (see Fig. 3). Even with this marked reduction in neutron throughput the use of this instrument on a high-flux reactor would produce data more quickly than a conventional instrument on a medium-flux reactor such as those at A.E.R.E.

If interplanar angles significantly greater than 35° are to be used it is apparent from Fig. 3 that the resolution does begin to suffer unacceptably. Reduction of the collimation to bring the resolution back to reasonable values decreases the transmission of the system to an extent which makes the instrument not competitive with conventional diffractometers on a reactor of lower flux.

The curves of Fig. 4 show the effect of increasing the monochromator take-off angle to 120°. This has the effect of increasing the angle of best focus so that a better resolution is obtained over a larger range of counter angle. The penalty that has to be paid for this

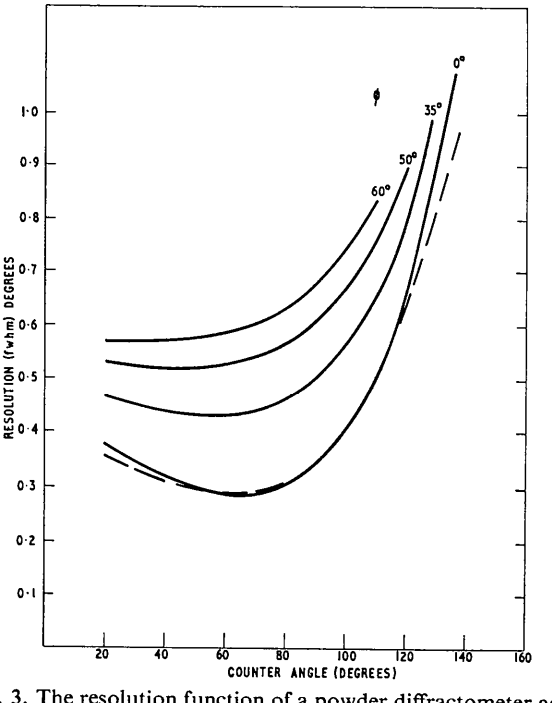

Fig. 3. The resolution function of a powder diffractometer as a function of interplanar angle, φ. The collimation angles are $\alpha_0=\alpha_2=15'$, $\alpha_1'=120'$, $\alpha_1=60'$. All $\beta=60'$, $\eta=\eta'=10'$, $\theta_M=45°$. The dashed line is the resolution function for $\varphi=35°$ with $\alpha_0=12'$, $\beta_1=30'$, $\alpha_2=7'$, all other divergencies as for the solid lines.

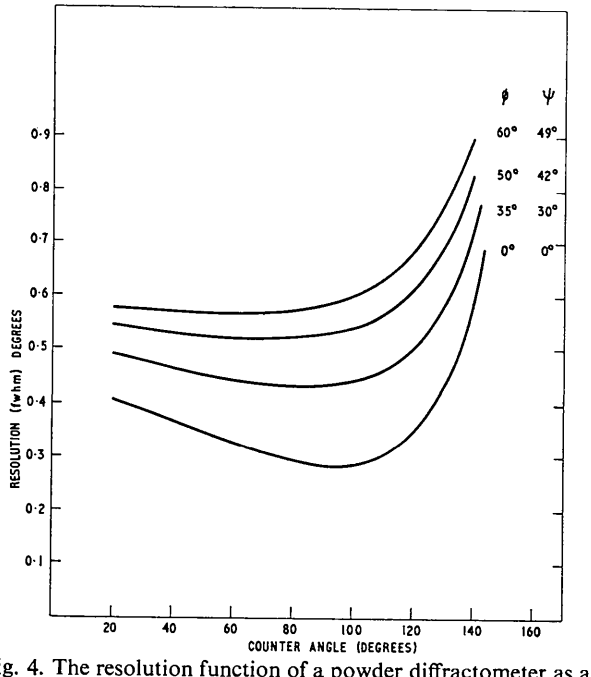

Fig. 4. The resolution function of a powder diffractometer as a function of interplanar angle, φ. The collimator and mosaic angles are as for Fig. 3, $\theta_M=60°$.

increased resolution is that the calculated transmission of the system is reduced to 0·6 times that of the 90° case.

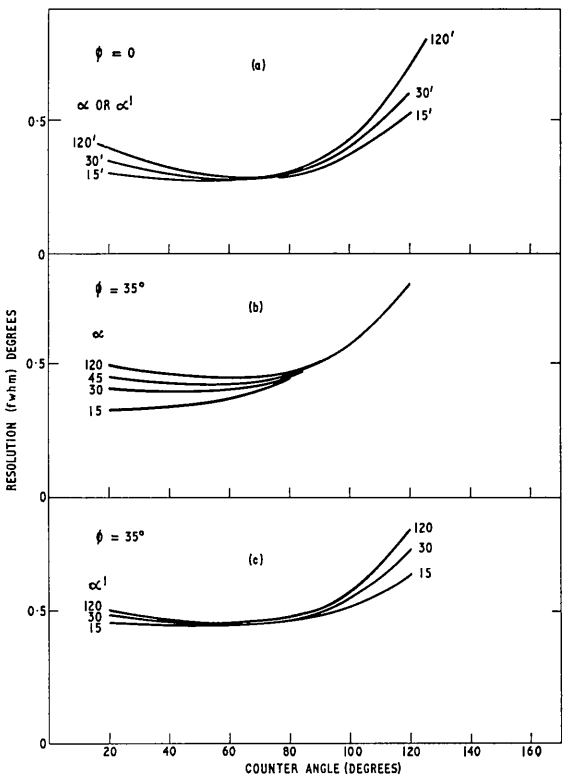

Fig. 5. The effect on the resolution of varying the collimation between monochromator and specimen. $\alpha_0=\alpha_2=15'$, $\beta'=60'$, $\eta=10'$, and $\theta_M=45°$. In (*a*) α_1 or α_1' is varied at $\varphi=0$; in (*b*) α_1 is varied at $\varphi=35°$ in (*c*) α_1 is varied at $\varphi=35°$.

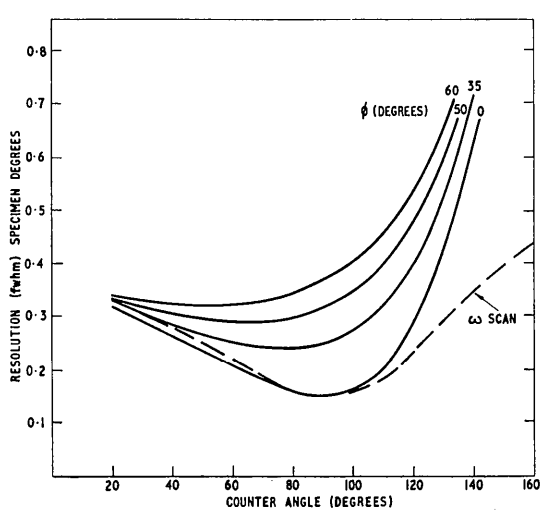

Fig. 6. The resolution function of a single-crystal diffractometer in the θ–2θ mode as a function of interplanar angle φ. Collimator angles are; $\alpha_0=\beta_0=30'$; $\alpha_1=\beta_1=34'$; $\alpha_1'=\beta_1'=120'$; $\alpha_2=\beta_2=60'$, $\eta_M=10'$, $\theta_M=45°$. The dashed line is the resolution function for the machine in the 'ω scan' mode.

It should be noted at this stage that at all monochromator take-off angles except 90° the value of interplanar angle φ is different from the inclination of the reactor neutron channel to the horizontal, ψ (see Appendix A).

An interesting point emerges from consideration of the effect of the collimation between monochromator and specimen on the resolution of the instrument. This is illustrated in Fig. 5 in which curves are drawn for various values of α_1 and α_1' keeping all other parameters constant. In Fig. 5(*a*) it can be seen that the effect at $\varphi=0$ of reducing α_1 or α_1' is to reduce the resolution width at small and large counter angles while keeping the points at the minimum of the curves constant. In Fig. 5(*b*) the same curves with $\varphi=35°$ are plotted with α varied and in 5(*c*) α_1' is varied with quite different results. Varying α_1 causes an effect at low counter angles and since this collimator acts in the specimen plane the results show the effect of collimation of the incident monochromatic beam on the resolution. Variation of α_1' on the other hand changes the collimation in the monochromator plane and thus alters the wavelength spread of the monchromatic beam on the specimen rather than its collimation. This has a greater effect on the region of large counter angles.

(ii) *Single-crystal diffractometer*

The calculated resolution widths in degrees of specimen rotation for a single crystal diffractometer working in the θ_s–$2\theta_s$ mode are given in Fig. 6. The dashed curve in this Figure is the peak width for the ω scan with $\varphi=0$. As the transmission of the system is independent of θ_s for the θ_s–$2\theta_s$ scan the deviation of this dotted curve from the solid line for $\varphi=0$ is a measure of the loss of counts experienced by keeping the counter in a fixed position.

The parameters of the diffractometer with resolution given in Fig. 6 are those that may be expected given the geometrical layout of the H.F.B.R. at Grenoble. In this reactor the inclined holes are arranged at an angle of 35° to the horizontal. The results obtained for $\varphi=35°$ may be improved to be comparable with those for $\varphi=0$ by decreasing the collimation angles producing a reduction of intensity to $\frac{1}{3}$ of the $\varphi=0$ values. Such a machine on an H.F.B.R. would have superior performance to a horizontal machine on a medium-flux reactor. Fig. 6 also shows that the single-crystal machine can be used with advantage on neutron channels at angles greater than 35°. Even with $\varphi=50°$ the resolution of the instrument having the parameters given in Fig. 6 has resolution nowhere worse than $2\frac{1}{2}$ times that of the horizontal machine and for $2\theta_s$ below 60° the ratio is less than a factor $1\frac{1}{2}$.

The reason why the increase of φ has a greater effect on a powder diffractometer than on a single-crystal diffractometer can be seen by considering the resolution matrix. When $\varphi=0$ the matrix reduces a half-value ellipsoid with one axis along the z direction. As the vertical collimation is usually more relaxed than the

horizontal collimation this vertical axis of the ellipsoid is usually larger than either of the other two axes. As φ is increased the major ellipsoid axis is tilted out of the vertical and it is reasonable to assume that the projection on the x axis, which produces the powder diffractometer width, will increase in length more rapidly than the distance between the points where the x axis cuts the ellipsoid, which produces the single-crystal width.

Finally in Fig. 7 are shown the curves for $\theta_M = 25°$ as this is another typical monochromator angle for single-crystal diffractometers. As before the results show that a loss of resolution of less than a factor $1\frac{1}{2}$ is found at $\varphi = 35°$ and less than $2\frac{1}{2}$ at $\varphi = 50°$.

Conclusions

This paper has investigated the resolution function of a two-axis diffractometer in which the monochromator and scattering planes are not coplanar. The results obtained indicate that a single-crystal diffractometer on an angled hole at up to 50° to the horizontal on an H.F.B.R. would be quite competitive with a conventional instrument on a medium-flux reactor. The results for a powder diffractometer are less favourable but a similar comparison indicates that holes up to 35° to the horizontal may still be used to produce a viable instrument.

I would like to thank Dr B. T. M. Willis for several stimulating discussions and for help with the presentation of the results. I would also like to thank Dr M. Cooper for a critical reading of the analysis and for several helpful suggestions.

APPENDIX A

Relationships between angles in real space

We define ψ as the angle of the reactor channel to the horizontal, and Ω as the angle between the line joining monochromator and specimen and the horizontal line perpendicular to the line of the reactor channel (see Fig. 1). With all other angles as defined previously we find:

$$\tan\psi = \tan\varphi\cos\Omega$$

and

$$\sin\psi = \sin\varphi\sin 2\theta .$$

These equations indicate that as Ω goes from $\pi/2$ to 0 to $-\pi/2$, φ ranges from $\pi/2$ to ψ to $\pi/2$ and 2θ goes from ψ to $(\pi-\psi)$.

APPENDIX B

As in CN we shall define sets of orthogonal axes $\mathbf{i}_1\mathbf{j}_1\mathbf{l}_1$, $\mathbf{i}_2\mathbf{j}_2\mathbf{l}_2$, $\mathbf{i}_0\mathbf{j}_0\mathbf{l}_0$, such that $\mathbf{i}_1$, $\mathbf{i}_2$ and $\mathbf{i}_0$ are parallel to $\mathbf{k}_I\mathbf{k}_F$ and $-\mathbf{Q}_0$ and $\mathbf{l}_1$, $\mathbf{l}_2$, $\mathbf{l}_0$ are vertical.

If $\Delta\mathbf{k}_i$ has components $x_1y_1'z_1'$ along $\mathbf{i}_1\mathbf{j}_1\mathbf{l}_1$ and $\Delta\mathbf{k}_f$ has components $x_2y_2z_2$ along $\mathbf{i}_2\mathbf{j}_2\mathbf{l}_2$ then we find

$$\Delta\mathbf{k}_i = (x_1\alpha + y_1'\beta)\mathbf{i}_0 + (-x_1\beta + y_1'\alpha)\mathbf{j}_0 + z_1'\mathbf{l}_0 \quad \text{(A1)}$$

$$\Delta\mathbf{k}_f = (-x_2\alpha + y_2\beta)\mathbf{i}_0 + (-x_2\beta - y_2\alpha)\mathbf{j}_0 + z_2\mathbf{l}_0 \quad \text{(A2)}$$

where $\beta = \cos\theta_s$, $\alpha = \sin\theta_s$ and for elastic scattering $x_2 = x_1$.

If we now rotate the monochromator scattering plane about $\mathbf{k}_I$ through an angle φ we may define $\Delta\mathbf{k}_i$ in terms of new variables $x_1y_1z_1$ which are related to $x_1y_1z_1$ by the equations $x_1 = x_1' = x$

$$\left.\begin{aligned} y_1' &= y_1\cos\varphi + z_1\sin\varphi \\ z_1' &= z_1\cos\varphi - y_1\sin\varphi \end{aligned}\right\} . \quad \text{(A3)}$$

Substituting into (A1) we obtain

$$\Delta\mathbf{k}_1 = (x_1\alpha + y'\delta\beta + z_1\gamma\beta)\mathbf{i}_0 + (-x\beta + y_1\alpha\delta + z_1\alpha\gamma)\mathbf{j}_0 + (z_1\delta - y_1\gamma)\mathbf{l}_0$$

where

$$\gamma = \sin\varphi,\ \delta = \cos\varphi .$$

Given

$$\Delta\mathbf{Q} = \Delta\mathbf{k}_f - \Delta\mathbf{k}_i = \Delta Q_x\mathbf{i}_0 + \Delta Q_y\mathbf{j}_0 + \Delta Q_z\mathbf{l}_0$$

$$\Delta Q_x = -2\alpha x + y_2\beta - y_1\delta\beta - z_1\gamma\beta$$

$$\Delta Q_y = -y_2\alpha - y_1\delta\alpha - z_1\alpha\gamma$$

$$\Delta Q_z = z_2 - z_1\delta + \gamma y_1 .$$

From these equations we find

$$y_2 = -\frac{\Delta Q_x}{2\beta} - \frac{\Delta Q_y}{2\alpha} + \frac{\alpha x_1}{\beta} = j + \frac{\alpha x}{\beta} \quad \text{(A4)}$$

$$y_1 = -\frac{\Delta Q_x}{2\beta\delta} - \frac{\Delta Q_y}{2\alpha\delta} - \frac{\alpha x}{\beta\delta} - \frac{\gamma}{\delta}z_1 = m + nx + pz_1 \quad \text{(A5)}$$

$$z_2 = \Delta Q_z + \frac{\gamma\Delta Q_x}{2\delta\beta} + \frac{\gamma\Delta Q_y}{2\alpha\delta} + \frac{z_1}{\delta} + \frac{\alpha\gamma x}{\beta\delta} = r + sz_1 + tx_1 . \quad \text{(A6)}$$

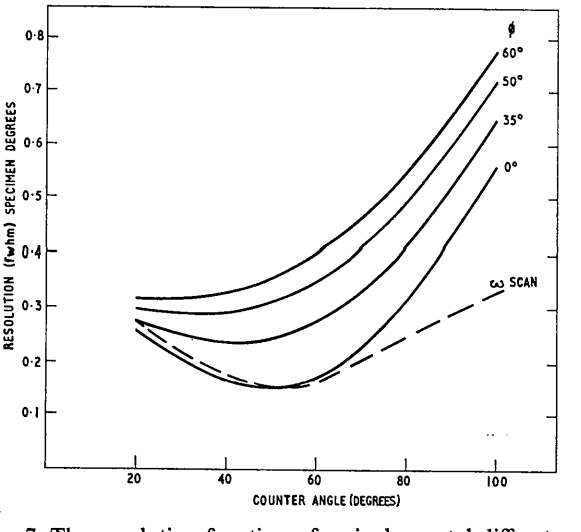

Fig. 7. The resolution function of a single-crystal diffractometer in the θ–2θ mode as a function of interplanar angle φ. The collimation is as for Fig. 6 but $\theta_M = 25°$.

We must also specify two variables y_3 and z_3 for the collimator C_1' which are equivalent to y_1 and z_1 of CN.

$$y_3 = -\frac{\Delta Q_x}{2\beta} - \frac{\Delta Q_y}{2\alpha} - \frac{\alpha x_1}{\beta} = W + \eta x_1 \qquad \text{(A7)}$$

$$z_3 = \frac{\gamma \Delta Q_x}{2\beta\delta} + \frac{\gamma \Delta Q_y}{2\alpha\delta} + \frac{z_1}{\delta} + \frac{\alpha\gamma}{\beta\delta}$$

$$\delta_1 = \sigma + sz_1 + tx_1 . \qquad \text{(A8)}$$

The transmission of the sytem is now similar to CN equation (17)

$$R \propto D \int \exp\left(-\tfrac{1}{2}[(ax+by_1)^2 + (cx+dy_1)^2 + ey_1^2 + fy_2^2 + gz_1^2 + hz_2^2 + e_1 y_3^2 + g_1 z_3^2]\right) \mathrm{d}x\,\mathrm{d}z_1$$

where

$$a = \frac{\tan\theta_M}{\eta_M k} \qquad b = \frac{1}{\eta_M k} \qquad c = 2\frac{\tan\theta_M}{\alpha_0 k}$$

$$d = \left(\frac{1}{\alpha_2 k}\right) \qquad e = \left(\frac{1}{\alpha_1 k}\right)^2 \qquad e_1 = \left(\frac{1}{\alpha_1' k}\right)^2$$

$$f = \left(\frac{1}{\alpha_2 k}\right)^2 \qquad g = \frac{1}{(4\sin^2\theta_M \eta_M' + \beta_0^2)k^2} + \left(\frac{1}{k\beta}\right)^2$$

$$g_1 = \left(\frac{1}{k\beta'}\right)^2 \qquad h = \left(\frac{1}{\beta_2 k}\right)^2 .$$

The values of y_1, y_2, y_3, z_2 and z_3 are given in equations (A4–A8); the α's and β's are the horizontal and vertical divergences of collimators C, and η and η' are the mosaic spreads of the monochromator in and perpendicular to the scattering plane. D ($\propto 1/\cos\varphi$) is the Jacobian of the transformation from y_1, y_2, z_2 to ΔQ_x, ΔQ_y, ΔQ_z. Then defining

$$A = b^2 + d^2 + e$$

$$B = ab + cd$$

$$J = \frac{(A + g_1 + h)}{2\beta\delta^2}\gamma$$

$$K = \frac{J\beta}{\alpha}$$

$$L = h/\delta$$

$$E = (A + g_1 + h)\alpha\gamma/2\beta\delta^2 + \beta\gamma/\delta$$

$$C = (A\gamma^2 + g_1 + h)/\delta^2 + g$$

$$F = a^2 + c^2 + \frac{[A + (g_1+h)\gamma^2]\alpha^2}{\beta^2\delta^2} + (e_1 + f)\frac{\alpha^2}{\beta^2} - \frac{2B\alpha}{\beta\delta}$$

$$Z = FC^2 - E^2 C$$

$$M = \frac{[A + (g_1+h)\gamma^2]\alpha}{2\beta^2\delta^2} + \frac{(e_1+f)}{2\beta^2}\alpha - \frac{B}{2\beta\delta}$$

$$N = \frac{[A + (g_1+h)\gamma^2]}{2\beta\delta^2} + \frac{(e_1+f)}{2\beta} - \frac{B}{2\alpha\delta}$$

$$P = \frac{h\alpha\gamma}{\beta\delta}$$

$$R = MC - JE$$

$$T = NC - KE$$

$$U = PC - LE ,$$

we find the transmission probability to be

$$R \propto D \sqrt{\frac{C}{Z}} \exp -\tfrac{1}{2} \sum_{i=1}^{3} \sum_{j=1}^{3} X_i A_y X_j$$

where

$$A_{11} = \frac{[A + (g_1+h)\gamma^2]}{4\beta^2\delta^2} + \frac{(e_1+f)}{4\beta^2} - \frac{J^2}{C} - \frac{R^2}{Z}$$

$$A_{22} = \frac{A + (g_1+h)\gamma^2}{4\alpha^2\delta^2} + \frac{e_1+f}{4\alpha^2} - \frac{K^2}{C} - \frac{T^2}{Z}$$

$$A_{33} = h - \frac{L^2}{C} - \frac{U^2}{Z}$$

$$A_{12} = \frac{A + (g_1+h)\gamma^2}{4\alpha\beta\delta^2} + \frac{(e_1+f)}{4\alpha\beta} - \frac{JK}{C} - \frac{RT}{Z}$$

$$A_{13} = \frac{h\gamma}{2\beta\delta} - \frac{JL}{C} - \frac{RU}{Z}$$

$$A_{23} = \frac{h\gamma}{2\alpha\delta} - \frac{KL}{C} - \frac{TU}{Z}, \qquad A_{ij} = A_{ji}$$

and $X_1 X_2 X_3$ are $\Delta Q_x \Delta Q_y$ and ΔQ_z.

References

CAGLIOTI, G., PAOLETTI, A. & RICCI, F. P. (1958). *Nucl. Instrum.* **3**, 223–228.

CAGLIOTI, G., PAOLETTI, A. & RICCI, F. P. (1960). *Nucl. Instrum. Meth.* **9**, 195–198.

COOPER, M. J. & NATHANS, R. (1968). *Acta Cryst.* A**24**, 481–448.